

Non-redox-active lipoate derivatives disrupt cancer cell mitochondrial metabolism and are potent anti-cancer agents in vivo

Zuzana Zachar^{1,3}, James Marecek², Claudia Maturo³, Sunita Gupta³, Shawn D. Stuart¹, Katy Howell³, Alexandra Schauble³, Joanna Lem³, Arin Piramzadian³, Sameer Karnik³, King Lee³, Robert Rodriguez³, Robert Shorr³ and Paul M. Bingham^{1,3,*}

¹Department of Biochemistry and Cell Biology

²Department of Chemistry

Stony Brook University

Stony Brook, New York

³Cornerstone Pharmaceuticals, Inc

Stony Brook, New York

and

Cranbury, New Jersey

Running Title: Lipoate analogs disrupt cancer metabolism

*corresponding author, pbingham@notes.cc.sunysb.edu, 516-909-7789

in press, Journal of Molecular Medicine

KEYWORDS: cancer, metabolism, mitochondria, lipoic acid, PDH

ABSTRACT: We report the analysis of CPI-613, the first member of a large set of analogs of lipoic acid (lipoate) we have investigated as potential anti-cancer agents. CPI-613 strongly disrupts mitochondrial metabolism, with selectivity for tumor cells in culture. This mitochondrial disruption includes activation of the well-characterized, lipoate-responsive regulatory phosphorylation of the E1 α PDH subunit. This phosphorylation inactivates flux of glycolysis-derived carbon through this enzyme complex and implicates the PDH regulatory kinases (PDKs) as a possible drug target. Supporting this hypothesis, RNAi knockdown of the PDK protein levels substantially attenuates CPI-613 cancer cell killing. In both cell culture and in vivo tumor environments, the observed strong mitochondrial metabolic disruption is expected to significantly compromise cell survival. Consistent with this prediction, CPI-613 disruption of tumor mitochondrial metabolism is followed by efficient commitment to cell death by multiple, apparently redundant pathways, including apoptosis, in all tested cancer cell lines. Further, CPI-613 shows strong anti-tumor activity in vivo against human non-small cell lung and pancreatic cancers in xenograft models with low side effect toxicity.

INTRODUCTION:

Development of more effective anti-cancer agents is expected to be aided greatly by recognizing the hallmarks of this disease most propitious as targets [1]. One especially attractive potential target set is cancer cell metabolism, well known to be extensively and characteristically altered in major tumor types [reviewed in 2-8].

In view of their scope and ubiquity, cancer-specific metabolic changes may present multiple targets for potentially selective and potent anti-cancer agents with broad spectrum efficacy. Moreover, the anti-cancer effects (and side effect toxicities) of agents targeting metabolism are expected to be mechanistically independent of those of current chemotherapies. The challenge is to identify viable approaches to capitalize upon these unique therapeutic opportunities.

Studies of cancer metabolism often focus on elevated glycolysis and reduced PDH activity. Nonetheless, persistence of significant PDH activity is vital to cancer cell survival, including for lipid biosynthesis and other functions (4-8). Figure 1a diagrams selected elements of mitochondrial metabolism, including the pyruvate dehydrogenase complex (PDH), a major supplier of acetyl-CoA to the TCA cycle. Specifically, PDH introduces glycolysis-derived pyruvate into the cycle where it can be oxidized to support ATP generation or its carbon diverted to anabolism. Anabolic diversion of TCA cycle intermediates requires additional replenishment of the cycle from other sources (anaplerosis). Glutamine conversion to TCA cycle intermediate alpha-ketoglutarate, introduced to the TCA cycle through the alpha-ketoglutarate dehydrogenase complex (KGDH), is an example of such anaplerosis.

PDH is one of only four enzymes using covalently joined lipoate as a catalytic cofactor. The other three enzymes using lipoate as a cofactor are KGDH, the branched chain oxo-acid dehydrogenase complex, BCOADH, and the glycine cleavage system, GCV (9-11). All four of these enzymes are found exclusively in the mitochondrial matrix. Moreover, KGDH is a TCA cycle enzyme, while BCOADH feeds amino acid-derived carbon into the TCA cycle.

Of these four lipoate-containing enzymes, PDH is uniquely central to mitochondrial carbon flow and its regulation is especially well understood. Moreover, the mechanisms involved in PDH regulation are unique to this complex among the four lipoate enzymes. Figure 1b illustrates the intermediates cyclically formed by covalently bound lipoate (lipoamide) during PDH catalysis. The relative levels of these catalytic intermediates reflect the saturation state of the enzyme [reviewed in 12-15]. Figure 1c shows a cartoon of how lipoate catalytic intermediates are thought to manage flux through the PDH complex, with high levels of the acyl and/or reduced lipoamide (indicating high PDH saturation) stimulating the PDH kinases (PDKs) to inactivate the E1 α PDH component by phosphorylation. These phosphorylation events block pyruvate entry into the complex [12-14]. Moreover, small, free lipoate-containing moieties can modulate these PDH regulatory processes in the purified enzyme in vitro [reviewed in 13-14].

The work of a number of investigators has defined the extensive reconfiguration of this lipoate-sensitive PDH regulatory machinery during malignant transformation. Four PDKs (PDK-1-4) regulate PDH by E1 α phosphorylation and each PDK has distinct regulatory properties, including its response to lipoate intermediates [reviewed in 15-16]. Moreover, at least two of the PDKs, PDK-1 and PDK-3, are up-regulated in response to the HIF pathway and often display substantially elevated levels in cancer cell lines and tumor biopsies [7, 17-22]. Thus, the lipoate-responsive PDK regulatory components of the PDH complex are substantially altered in tumor

cells relative to the corresponding normal cell machinery and the reaction of tumor cell PDH to lipoate status is likely to be significantly changed.

These known cancer specific changes are likely to reflect a larger body of tumor alterations in PDH regulation, as yet uncharacterized. Moreover, it is possible, though currently unexplored, that some or all of the other three lipoate-containing enzymes are also regulated differently in tumor cells than in normal cells.

Thus, lipoate occupies a unique position in cancer biology. In addition to its catalytic roles, it is a regulatory molecule with a small, specific repertoire of mitochondrial functions, including modulation of at least one key metabolic enzyme whose lipoate-sensitive regulation is remodeled in cancer cells. Further, it is plausible that these and other lipoate-dependent regulatory functions can be manipulated by exogenously supplied molecules.

These observations suggest that systemically delivered lipoate analogs might selectively disrupt cancer mitochondrial metabolism, potentially resulting in cancer cell death. We report a series of results strongly supporting this hypothesis and indicating that a specific lipoate analog, CPI-613, represents a potentially useful new anticancer agent.

MATERIALS AND METHODS:

CPI-613 chemistry

CPI-613 was synthesized from D,L lipoate. Synthetic details, NMR structure confirmation and purity information are in Supplemental Material.

Cells

Cells were obtained from ATCC or commercial providers (Supplemental Material). All experiments initiated at cell densities of ca. 50% confluence. Except as noted all experiments were performed with NCI-H460 NSCLC human tumor cells.

Tumor growth inhibition studies

Studies used CD1-Nu/Nu female mice inoculated with tumor cells on the dorsal flank and treated by intraperitoneal injection of drug as described in the legend to Figure 7 and Supplemental Material. All studies were carried out according to Stony Brook University IACUC standards for ethical treatment of animals.

Cell death assays

For most assessments of cell viability CellTiter-Glo assay (Promega), based on total cellular ATP levels, was used at times sufficiently long not to be confounded by early, reversible CPI-613-induced reduction in ATP levels (typically 24 hours in pyruvate medium and 36-48 hours in glucose medium; see, Figures 3a-c).

Membrane permeable, esterase-sensitive methyl-pyruvate (Sigma) was used to deliver pyruvate as a carbon source.

Quantifying execution of different cell death pathways in Figure 6 employed preferential DAPI uptake by dying cells and resulting stained nuclear morphology. See text and Supplemental Material for additional details.

ATP assay

Cells were plated in 12 well plates at 200,000 cells/well or 35mm dishes at 250,000 cells per dish. 18-25 hours later, medium was replaced with fresh medium containing drug solvent (dimethylformamide) with or without drug for time intervals and at drug concentrations as indicated in the Figures in the main text. [Cell viability and integrity was assessed by recovery of ATP levels after drug withdrawal and by trypan blue exclusion in selected cases.] ATP was measured using CellTiter-Glo luminescence assay (Promega) according to manufacturer's directions. All measurements were performed in triplicate and showed high consistency. Mean \pm standard error of the mean (SEM) were calculated and graphically presented (SigmaPlot). Methyl pyruvate medium in Figures 3 and 4 consisted of RPMI without glucose (Invitrogen), supplemented with 10% dialyzed fetal bovine serum, 5mM HEPES (pH 7.4) and 10mM methyl pyruvate. The matched glucose medium was conventional RPMI (Invitrogen).

E1 α phosphorylation

Cell lysates were processed using the Zoom Benchtop proteomics system (Invitrogen). Filter transfers were assayed with commercial Abs (Invitrogen and EMD). See Supplemental Material for additional details.

CO₂ release through carbon source oxidation

Oxidative release of carbons as carbon dioxide from glucose was assayed by filter capture as described in [23] with minor modifications. See Supplemental Material for additional details.

JC-1 potentiometric dye measurement of mitochondrial membrane potential

The dye JC-1 (5,5,6,6-tetrachloro-1,1,3,3-tetraethylbenzimidazolylcarbocyanine iodide) was used to measure mitochondrial membrane potential essentially as described in [24]. This dye is imported into mitochondria in a potential dependent manner. As the dye concentrates in mitochondria it forms aggregates which fluoresce red (590nm). When the dye is released from depolarized mitochondria it is diluted in the cytosol and forms monomers fluorescing green (485nm). FACS measurement of the red/green fluorescence spectrum of treated cells allows direct measurement of mitochondrial membrane potential. See Supplemental Material for additional details.

RNAi PDK knockdowns

H460 cells were transfected with a mixture of siRNAs against all four PDKs or scrambled sequence control for 12 hours and treated with 200 μ M CPI-613 for an additional 17 hours followed by analysis of cell death as above. Levels of PDK protein knockdown were determined by Western analysis as described in Supplemental Material.

Statistical analysis

All data were expressed as mean \pm SEM. Data were analyzed by ANOVA (mouse studies) or Students t test. p values ≤ 0.05 were considered significant.

RESULTS:

Lipoate derivative, CPI-613, efficiently kills tumor cells in culture

CPI-613 is a lipoate derivative synthesized to be catalytically inert but to potentially mimic lipoate catalytic intermediates (Figure 1d). CPI-613, but not the parental lipoate compound, efficiently kills every tumor cell line we have tested in the dose range examined (Figure 2a-c). Moreover, diverse tested normal cells are significantly less sensitive to CPI-613 (Figure 2b).

The series of tumor cell lines listed in Figure 2c carry an array of different oncogene mutations as indicated, as well as diverse mutational alterations in cell death machinery [reviewed in 25]. These genetic changes apparently produce differences in sensitivity to traditional agents, including taxanes, of several orders of magnitude, while CPI-613 sensitivity varies only modestly (Figure 2c).

CPI-613 strongly disrupts mitochondrial metabolism, including inhibition of PDH function

Culturing cancer cells in medium replacing glucose, a glycolytic substrate, with pyruvate, a mitochondrial substrate, constrains them to carry out net ATP synthesis through mitochondrial pathways, the TCA cycle and oxidative phosphorylation. This modification has little effect on the ultimate sensitivity of tested cancer cell lines to CPI-613 killing (Figure 2a). However, this change to exclusively mitochondrial carbon sources has substantial and informative effects on the kinetics of the CPI-613 response as follows.

When H460 human lung cancer cells are cultured in medium containing pyruvate and glutamine as the predominant carbon sources, ATP levels are substantially reduced within less

than 60 minutes in response to CPI-613 treatment (Figure 3a). Moreover, this reduction in ATP levels is initially reversible; a large majority of cells remain viable and recover normal ATP levels if the drug is removed within two hours (Figure 3a; Supplemental Material). After longer treatment times, cells become irreversibly committed to death and execute cell death as assessed by propidium uptake and annexin staining (Figure 3a; also see below).

The more rapid onset of commitment to cell death in pyruvate than in glucose (Figure 3a and b) suggests that cell death is pursuant to mitochondrial inhibition and that shuttling of ATP and/or reducing potential from cytosolic glycolysis into the mitochondrion (9) delays commitment to cell death. Supporting this hypothesis, we observe that even mild perturbation of glycolysis with low doses of the glyceraldehyde phosphate dehydrogenase inhibitor, iodoacetate, prevents glucose from forestalling CPI-induced early reductions in ATP levels (Figure 3c).

We used metabolic flux measurements to directly assess the effects of CPI-613 on PDH activity, a potential component of the drug's mitochondrial effects. The 3 and 4-carbons of glucose become the 1-carbon of pyruvate generated by glycolysis. The pyruvate 1-carbon is released as carbon dioxide almost exclusively as a result of PDH function (Figure 1b). Thus, measuring carbon dioxide release when cells are pulse-labeled with 3,4-¹⁴C glucose allows assessment of PDH function [23](Figure 3d).

This ¹⁴CO₂ release assay indicates that CPI-613 inhibits PDH function in a time- and drug dose-dependent fashion in tumor cells (Figure 3e). Note that under these conditions (glucose as a major carbon source) CPI-613 induces only very limited cancer cell death during the 8-hour assay interval (Figure 3b). Thus, this inhibition of PDH is likely to be an acute effect of the drug, rather than a downstream consequence of cell death commitment or execution.

Moreover, CPI-613 differentially inhibits PDH activity in normal and tumor cells. Low doses of CPI-613 mildly *stimulate* pyruvate oxidation in normal cells, with higher doses producing only transient, reversible inhibition (Figure 3e).

Disruption of mitochondrial metabolism is accompanied by loss of mitochondrial membrane potential (24 and references therein). Thus, if CPI-613 is disrupting tumor cell mitochondrial metabolism, mitochondrial membrane potential should decline. Figure 4 shows that CPI-613 significantly reduces mitochondrial membrane potential as assessed by a JC-1 localization assay. Moreover, this loss of membrane potential is initially reversible, becoming irreversible later (Figure 4b), concomitantly with commitment to cell death (Figure 3a).

CPI-613 induces extensive regulatory phosphorylation of tumor cell PDH and RNAi knockdown of PDK protein levels strongly attenuates drug induced cell death

Results in Figure 3e indicate that cancer cell PDH function is acutely inhibited by CPI-613. In view of the documented lipoate-sensitive regulatory properties of the PDH complex, one candidate for the basis of this effect is CPI-613 stimulation of PDK activity. PDK activation, in turn, results in phosphorylation of the E1 α subunit inactivating PDH activity (Figure 1c).

At three hours of drug treatment in glucose-containing medium 80-90% of cells remain fully viable if drug is withdrawn (Figures 3b and 5d; Supplemental Material). Under these same treatment conditions, E1 α becomes highly post-translationally modified as assessed by two-dimensional Western gel analysis (Figure 5a and b). This timing indicates that PDH E1 α post-translational modification precedes commitment to cell death. Moreover, this post-translational modification includes large increases in the levels of all three major phospho-epitopes known to

result from PDK regulatory phosphorylation of PDH E1 α (Figure 4c). Finally, this extensive CPI-613-induced phosphorylation of PDH E1 α is selective for tumor cells (Figure 5b).

These observations suggest that CPI-613 interaction with tumor cell-remodeled PDK regulatory phosphorylation may be central to the cancer cell drug response. We tested this possibility by knocking down PDK levels in H460 tumor cells. Knockdowns of individual PDKs had only limited effect (results not shown). However, concurrent knockdown of all four PDKs produced very robust protection from CPI-613 killing (Figure 5e), indicating that PDKs are essential for the tumor cell response to CPI-613.

CPI-613 induces multiple, redundant cell death pathways

Mitochondria are centrally involved in decision making for various cell death pathways [see 26, for example]. Moreover, disruption of mitochondrial metabolism by non-cancer selective agents has been widely reported to produce cell death [see, for example, 27]. Thus, we assessed the nature of the cell death pathways induced by CPI-613 treatment.

Initially we observed apoptotic cell death in a significant fraction of H460 cells, based on cell morphology as well as regulatory cleavage of caspase-3 and PARP (Figures 6a and b and Supplemental Figure S1). However, blockage of apoptotic pathways with the pan-caspase inhibitor z-VAD-FMK produced no significant protection against CPI-613-induced death. We therefore exploited a simple dye uptake/nuclear morphology assay to assess the cell death pathway executed by large numbers of individual cells in treated populations.

Apoptotic cells have well defined nuclear sub-inclusions and characteristic plasma membrane blebbing (Figure 6a; Movie #1 in Supplemental Material). In contrast, non-apoptotic dying cells display uniform nuclear staining (Figure 6a) accompanied by extrusion of large

plasma membrane projections (Movie #2 in Supplemental Material). CPI-613 induces apoptotic and non-apoptotic cell death in both H460 carcinoma and Saos-2 sarcoma cell lines (Figures 6b and c) resulting in death of all cells. z-VAD-FMK efficiently suppresses apoptosis in both cell lines. Moreover, under this suppression of apoptosis, all CPI-613-treated cells still die, but do so exclusively by non-apoptotic pathways (Figures 6b and c).

CPI-613 has potent anti-cancer activity in human tumor xenograft models

Figure 7 shows effects of CPI-613 in a nude mouse human tumor xenograft model of a pancreatic tumor cell (BxPC-3) and a non-small cell lung tumor cell (H460). Drug treatment produces robust BxPC-3 tumor growth inhibition (panel 7a). Moreover, all untreated tumor-bearing animals expired within three months (panel 7b). In contrast, over 40% of treated animals survived until the experiment was terminated at over eight months (259 days; panel 6c). A substantial fraction of long term mortality of the treated animals resulted from euthanasia of individuals suffering from ulceration of self-inflicted wounds (according to IACUC approved policies and protocols). This source of mortality is characteristic of these immunocompromised animals and was apparently unrelated to their xenografts. Collectively, these observations indicate substantial long term, post-treatment suppression of this human pancreatic tumor in a substantial fraction of CPI-613 treated animals.

Similarly, CPI-613 produced strong tumor growth inhibition of H460 human non-small cell lung carcinoma at 10mg/kg (Figure 7c). The maximum tolerated dose in mice for CPI-613 is ca.100mg/kg under the conditions of this study. Thus, CPI-613 shows strong anti-cancer activity at well-tolerated doses.

Consistent with this low side-effect toxicity, extensive toxicology and hematotoxicity studies in large animal models (performed under contract by Charles River Laboratories; Wilmington, MA, USA) indicate that CPI-613 produces little or no side effect toxicity in expected therapeutic dose ranges and is well tolerated even at very high doses (manuscript in preparation; See Supplemental Material for one representative example from this extensive data set).

DISCUSSION

Lipoate analog, CPI-613, severely disrupts tumor cell mitochondrial metabolism as assessed by its impact on ATP levels (Figure 3a) and mitochondrial membrane potential (Figure 4) in pyruvate-glutamine medium.

CPI-613 perturbation of tumor cell mitochondrial metabolism includes substantial inhibition of tumor PDH activity as assessed by metabolic flux analysis (Figure 3e) correlating with very extensive regulatory phosphorylation of the E1 α subunit (Figure 5a-c). Moreover, this phosphorylation is selective for tumor cell PDH (Figure 5b) and includes high levels of induction of the specific phospho-epitopes produced by the lipoate-sensitive PDK kinases regulating PDH activity (Figure 5c). This population of PDK kinases is quantitatively and possibly qualitatively remodeled in the course of malignant transformation (7, 17-22). RNAi knockdown of the PDK population substantially protects H460 tumor cells from CPI-613 killing (Figure 5e) directly implicating these kinases in the drug response.

The three other lipoate-dependent enzymes, all mitochondrial, may also be remodeled in their regulatory response to lipoate in cancer cells. These may also represent potential tumor-specific CPI-613 targets, an important subject for future investigation.

CPI-613 induction of commitment to cell death follows initial disruption of mitochondrial metabolism (Figure 3a). Moreover, the concomitant delay in CPI-613-induced reduction in ATP levels and commitment to cell death in the presence of glucose indicates that cell death induction correlates intimately with drug effects on mitochondrial metabolic status (Figures 3a-c).

Most tumor cells substantially down-regulate fatty acid oxidation, an alternative source of TCA acetyl-CoA (9). Moreover, for glutaminolysis alone to fully maintain mitochondrial metabolism depends on the anaplerotic reaction of maleic enzyme (using glutaminolysis-derived malate) to generate pyruvate which must reenter the TCA cycle through PDH (9). Thus, inhibition of PDH activity in tumor cells could account, in part or entirely, for the profound effects on mitochondrial energy metabolism we observe. In view of the vital role of mitochondrial function in sustaining cell survival, even in hypoxic, glycolytic solid tumor cells *in vivo*, severe inhibition of mitochondrial metabolism is expected to induce cancer cell death, as we observe.

Cancer cell death ensuing from CPI-613 treatment results from the activation of apoptosis in a subset of cells in the treated population and non-apoptotic death in the remaining cells (Figure 6). Moreover, inhibition of apoptosis in treated cell populations results in universal death by one or more non-apoptotic pathways (Figure 6). These observations indicate that CPI-613 induces multiple, redundant cell death pathways in tested cancer cell lines. Further, CPI-613 is

comparably effective in inducing cell death in all tested cancer cells, irrespective of extensive, diverse genotypic variation.

Collectively, our results indicate that the CPI-613 disrupts tumor cell mitochondrial metabolism. Moreover, the unique and central role of lipoate in tumor-specific metabolism suggests that these properties may have significant clinical value. No other characterized agents targeting cancer metabolism acts as we observe for CPI-613 [reviewed in 28-29]. Note specifically that CPI-613 has diametrically opposite effects from recently described agents that attempt to undo cancer-specific PDH regulation and thereby up-regulate PDH function in tumor cells, including dichloroacetate (DCA) and molecules antagonizing HIF activation [30; reviewed in 8]. In contrast, CPI-613 may kill cancer cells by hyper-stimulation of, rather than opposition to, tumor-specific PDH regulatory processes.

Apparently as a result of these novel properties, CPI-613 shows potent anticancer effects against a pancreatic and non-small cell human tumor in *in vivo* xenograft models (Figure 7). These observations further indicate that CPI-613 has potentially useful new properties as an anticancer agent attacking tumor cell-specific metabolism.

ACKNOWLEDGEMENTS AND DISCLOSURE STATEMENT

We are grateful to Gregg Semenza and Bob Weinberg for helpful discussions. We thank colleagues, including Pat Hearing, for help early in this project. This work was largely funded by Cornerstone Pharmaceuticals with early support from the Carol M. Baldwin Breast Cancer Research Fund and the Stony Brook Center for Biotechnology. Maturo, Gupta, Howell,

Schauble, Lem, Piramzadian, Karnik and Lee are or were employees of Cornerstone Pharmaceuticals, developers of CPI-613. Zachar, Rodriguez, Shorr and Bingham have a financial interest in Cornerstone Pharmaceuticals.

REFERENCES:

1. Hanahan D, Weinberg RA (2011) Hallmarks of cancer: The next generation. *Cell* 144: 646-674.
2. Baggetto LG (1992) Deviant energetic metabolism of glycolytic cancer cells. *Biochimie* 74: 959-974.
3. Christofk H R, Vander Heiden MG, Harris MH, Ramamathan A, Gerszten RE, Wei R, Flemming MD, Schreiber SL, Cantley LD (2008) The M2 splice isoform of pyruvate kinase is important for cancer metabolism and tumour growth. *Nature* 452: 230-234.
4. DeBerardinis RJ, Lum JJ, Hatzivassiliou G, Thompson CB (2008a) The biology of cancer: Metabolic reprogramming fuels cell growth and proliferation. *Cell Metab* 7: 11-20.
5. DeBerardinis RJ, Sayed N, Ditsworth D, Thompson, CB (2008b) Brick by brick: metabolism and tumor cell growth. *Curr Opin Genet Dev* 18: 54-61.
6. Vander Heiden MG, Cantley LC, Thompson CB (2009) Understanding the Warburg effect: The metabolic requirements of cell proliferation. *Science* 324: 1029-1033.
7. Semenza GL (2009) Regulation of cancer cell metabolism by hypoxia-inducible factor 1. *Semin Cancer Biol* 19: 12-16.

8. Cairns RA, Harris IS, Mak TW (2011) Regulation of cancer cell metabolism. *Nat Rev Cancer* 11: 85-95.
9. Garrett R, Grisham CM (2007) *Biochemistry*. Thomson Brooks/Cole, Southbank, Vic., Australia; Belmont, CA).
10. Kikuchi G, Motokawa Y, Yoshida T, Hiraga K (2008). Glycine cleavage system: reaction mechanism, physiological significance, and hyperglycinemia. *Proceedings of the Japan Academy Series B-Physical and Biological Sciences* 84: 246-263.
11. Yeaman SJ (1989). The 2-oxo acid dehydrogenase complexes - Recent advances. *Biochemical Journal* 257: 625-632.
12. Roche TE, Baker JC, Yan YH, Hiromasa R, Gong XM, Peng T, Dong JC, Turhan A, Kastaen Sa (2001) Distinct regulatory properties of pyruvate dehydrogenase kinase and phosphatase isoforms. *Prog Nucl Acid Res and Mol Biol* 70: 33-75.
13. Bunik VI (2003) 2-oxo acid dehydrogenase complexes in redox regulation: Role of the lipoate residues and thioredoxin. *Euro J Biochem* 270: 1036-1042.

14. Roche TE, Hiromasa Y, Turkan A, Gong X, Peng T, Yan X, Kasten SA, Bao H, Dong J (2003) Essential roles of lipoyl domains in the activated function and control of pyruvate dehydrogenase kinases and phosphatase isoform 1. *Euro J Biochem* 270: 1050-1056.
15. Sugden MC, MJ Holness (2003) Recent advances in mechanisms regulating glucose oxidation at the level of the pyruvate dehydrogenase complex by PDKs. *Am J Physiol* 284: E855-E862.
16. Roche TE, Hiromasa Y (2007) Pyruvate dehydrogenase kinase regulatory mechanisms and inhibition in treating diabetes, heart ischemia, and cancer. *Cell Mol Life Sci* 64: 830-849.
17. Koukourakis MI, Giatromanolaki A, Giatromanolaki A, Sivridis E, Gatter KC, Harris AL (2005) Pyruvate dehydrogenase and pyruvate dehydrogenase kinase expression in non small cell lung cancer and tumor-associated stroma. *Neoplasia* 7: 1-6.
18. Kim JW, Tchernyshyov I, Semenza GL, Dang CV (2006) HIF-1-mediated expression of pyruvate dehydrogenase kinase: A metabolic switch required for cellular adaptation to hypoxia. *Cell Metab* 3: 177-185.
19. Papandreou I, Cairns RA, Fontana L, Lim AL, Denko NC (2006) HIF-1 mediates adaptation to hypoxia by actively downregulating mitochondrial oxygen consumption. *Cell Metab* 3: 187-197.

20. Denko NC (2008) Hypoxia, HIF1 and glucose metabolism in the solid tumour. *Nat Rev Cancer* 8: 705-713.

21. McFate T, Mohyeldin A, Mohyeldin A, Lu H, Thakar J, Henriquez J, Halim ND, Wu H, Schell MJ, Tsang TM, Teahan O, Zhou S, Califano JA, Jeoun NH, Harris RA, Verma A. (2008) Pyruvate dehydrogenase complex activity controls metabolic and malignant phenotype in cancer cells. *J Biol Chem* 283: 22700-22708.

22. Lu CW, Lin SC, Chen KF, Lai YY, Tsai SJ (2008) Induction of pyruvate dehydrogenase kinase-3 by hypoxia-inducible factor-1 promotes metabolic switch and drug resistance. *J Biol Chem* 283: 28106-28114.

23. Schafer Z T, Grassian AR, Song LL, Jiang ZY, Gerhart-Hines Z, Irie HY, Gao SZ, Puigserver P, Brugge, JS (2009) Antioxidant and oncogene rescue of metabolic defects caused by loss of matrix attachment. *Nature* 461: 109-114.

24. Takeda Y, Perez-Pinzon MA, Ginsberg MD, Sick TJ (2004) Mitochondria consume energy and compromise cellular membrane potential by reversing ATP synthetase activity during focal ischemia in rats. *J Cereb Blood Flow Metab* 24: 963-992.

25. de Bruin EC, Mederna JP (2008) Apoptosis and non-apoptotic deaths in cancer development and treatment response. *Cancer Treat Rev* 34: 737-749.
26. Nagley P, Higgins GC, Higgins GC, Atkin JD, Beart PM (2010) Multifaceted deaths orchestrated by mitochondria in neurons. *Biochim Biophys Acta* 1802: 167-185.
27. Skulachev VP (2004) Wages of Fear: transient threefold decrease in intracellular ATP level imposes apoptosis. *Biochim Biophys Acta* 1658: 141-147.
28. Cuezva JM, Ortega AD, Willer I, Sanchez-Cenizo L, Aldea M, Sanchez-Arago M (2009) The tumor suppressor function of mitochondria: Translation into the clinics. *Biochim Biophys Acta* 1792: 1145-1158.
29. Tennant DA, Duran RV, Gottlieb E (2010) Targeting metabolic transformation for cancer therapy. *Nat Rev Cancer* 10: 267-277.
30. Bonnet S, Archer SL, Allalunic-Turner J, Harmony A, Beaulieu C, Thompson R, Lee CT, Lopaschuk GD, Puttagunta L, Bonnet S, Harry G, Hashimoto K, Porter, CJ, Andrade MA, Thebaud B, Mechelas ED (2007) A mitochondria-K⁺ channel axis is suppressed in cancer and its normalization promotes apoptosis and inhibits cancer growth. *Cancer Cell* 11: 37-51.
31. Ikediobi ON, Davies H, Bignell G, Edkins S, Stevens C, O'Meara S, Santarius R, Avis T, Barthrope S, Brackenbury L, Buck G, Butler A, Clements J, Cole J, Dicks E, Forbes S, Gray K,

Halliday K, Harrison R, Hills K, Hinton J, Hunter C, Jenkinson A, Jones D, Kosmidou V, Lugg R, Menzies A, Mironenko T, Parker A, Perry J, Raine K, Richardson D, Shepherd R, Small A, Smith R, Solomon H, Stephens P, Teague J, Tofts C, Varain J, Webb T, West S, Widaa S, Yates A, Reinhold W, Weinstein JN, Stratton MR, Futreal PA, Wooster R (2006) Mutation analysis of 24 known cancer genes in the NCI-60 cell line set. *Mol Cancer Ther* 5:2606-2612.

32. Rodrigues AR, Rowan A, Smith MEF, Kerr IB, Bodmer WF, Gannon JV, Lane DP (1990) p53 mutations in colorectal cancer. *Proc Natl Acad Sci, USA* 87: 7555-7559.

33. Augenlicht, LH, Wadler S, Corner G, Richards C, Multani AS, Pathak S, Benson A, Haller D, Heerdt BG (1997) Low-level c-myc amplification in human colonic carcinoma cell lines and tumors: A frequent p53-independent mutation associated with improved outcome in randomized multi-institutional trial. *Cancer Res* 57: 1769-1775.

FIGURES:

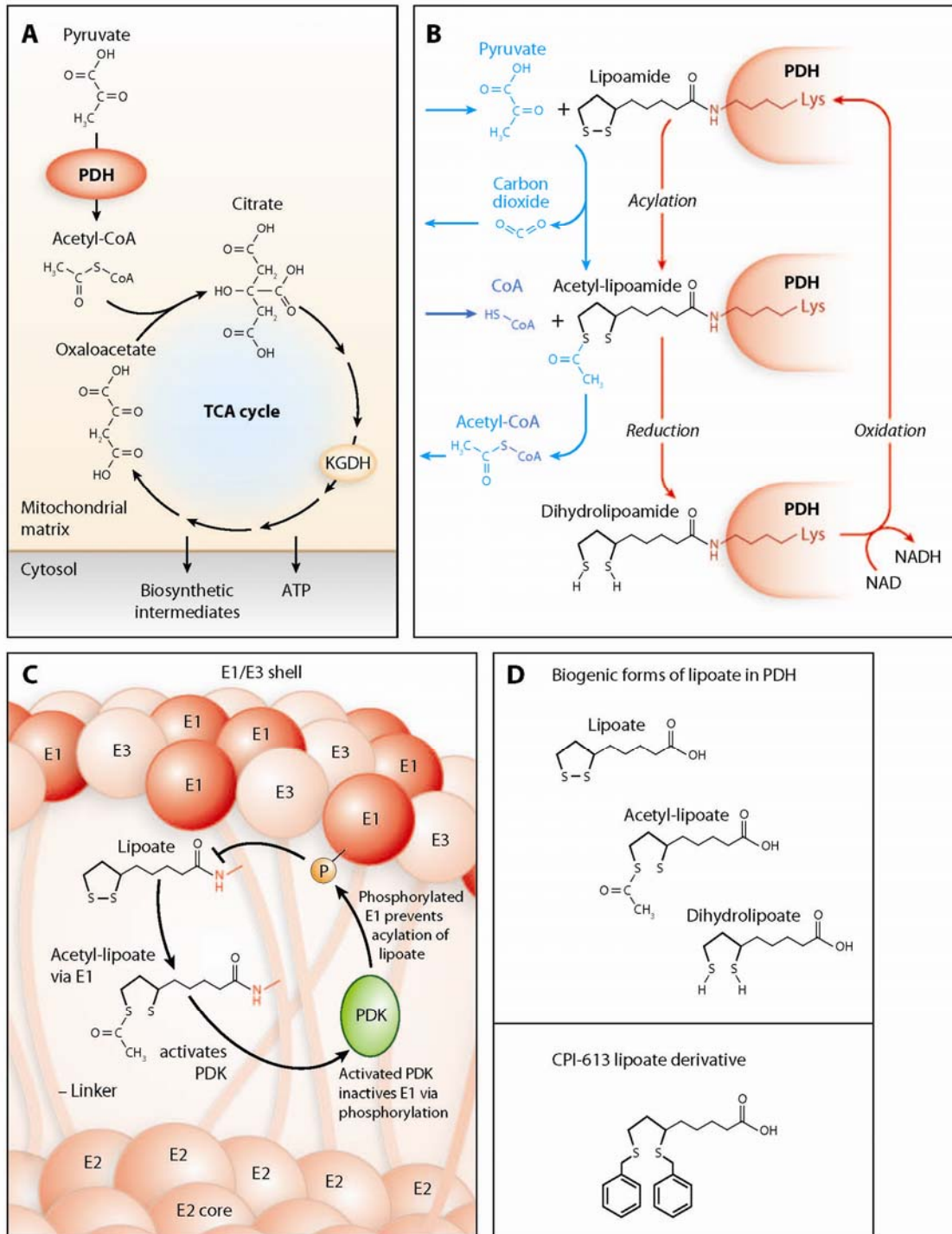
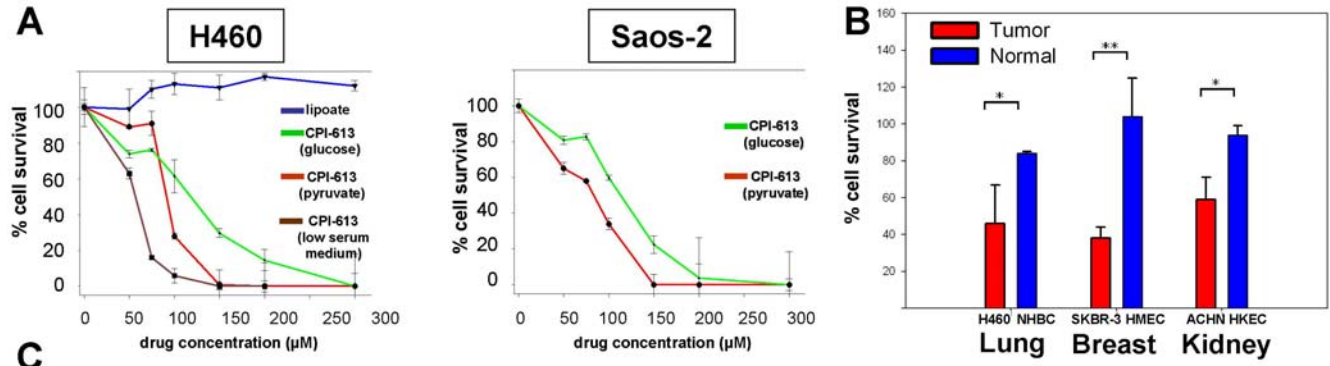


Figure 1

Figure 1: *Lipoate-containing enzyme, pyruvate dehydrogenase (PDH), is central to cancer mitochondrial metabolism and metabolic regulation and CPI-613 resembles PDH lipoate catalytic intermediates with regulatory function.* **a.** Illustrates selected details of the TCA cycle. PDH channels glucose-derived carbon (pyruvate) into the TCA cycle, supporting production of ATP and biosynthetic intermediates. **b.** Illustrates the cyclic acetylation/reduction of lipoate during its catalytic functions in the PDH complex. **c.** Depicts lipoate- (lipoamide-) sensitive regulation of the PDH complex. Acylation-reduction state of lipoate modulates PDH activity by regulating PDKs that inactivate the PDH E1 α subunit by phosphorylation. **d.** Shows biogenic lipoate catalytic intermediates and the CPI-613 lipoate analog.



Cancer cell origin	Cell line	Gene mutation ^a							Gene overexpression		EC 50 (uM)
		CDKN2A	PI3K	PTEN	KRAS	RB1	STK11	TP53	<u>Myc</u>	<u>MDR1</u>	
BONE osteosarcoma	Saos-2					X ^b					120
BREAST adenocarcinoma	MCF-7	X	X								280
BREAST adenocarcinoma	NCI/ADR-RES							X		↑	280
COLORECTAL carcinoma	SW-480							X ^c	↑ ^d		220
KIDNEY carcinoma	H498	X		X							200
KIDNEY carcinoma	ACHN	X									220
LUNG carcinoma (NSCLC)	A549	X			X		X				100
LUNG carcinoma (NSCLC)	H460	X	X		X		X				120
LUNG carcinoma (SCLC)	NCI/H69		X			X		X			150
MUSCLE rhabdomyosarcoma	RD				X			X			200
OVARIAN adenocarcinoma	A2780			X							230
OVARIAN adenocarcinoma	A2780Dx			X						↑	240
PANCREATIC adenocarcinoma	BxPC-3	X						X			120
PROSTATE adenocarcinoma	PC-3			X				X			150
UTERINE sarcoma	MES-SA	X									150
UTERINE sarcoma	MES-SA/MX2	X								↑	150

Figure 2

Figure 2: *CPI-613 is selectively toxic for all tested tumor cells in culture.* **a.** Shows representative examples of dose-response determinations for cell killing by CPI-613 in H460 human lung cancer cells and Saos-2 human sarcoma cells in RPMI medium (glucose) or RPMI medium in which glucose was replaced by pyruvate. Also shown is CPI-613 killing in the defined, low serum NHBC growth medium employed in Figure 3e. Albumin binds CPI-613 (unpublished results) and the potency of CPI-613 is higher in this low serum medium. **b.** Shows differences in CPI-613 killing of matched pairs of tumor and normal (primary) cells treated with drug near the EC_{50} . * $p < 0.018$; ** $p < 0.001$. **c.** Tabulates EC_{50} 's and selected details of tissue of origin, tumor type and genotype of tested cancer cells. *Information on mutations compiled from the COSMIC data base <http://www.sanger.ac.uk/genetics/CGP/cosmic/>; [31]. ^{\$}denotes gene is mutant in cell line. [#][32]. [&][33]

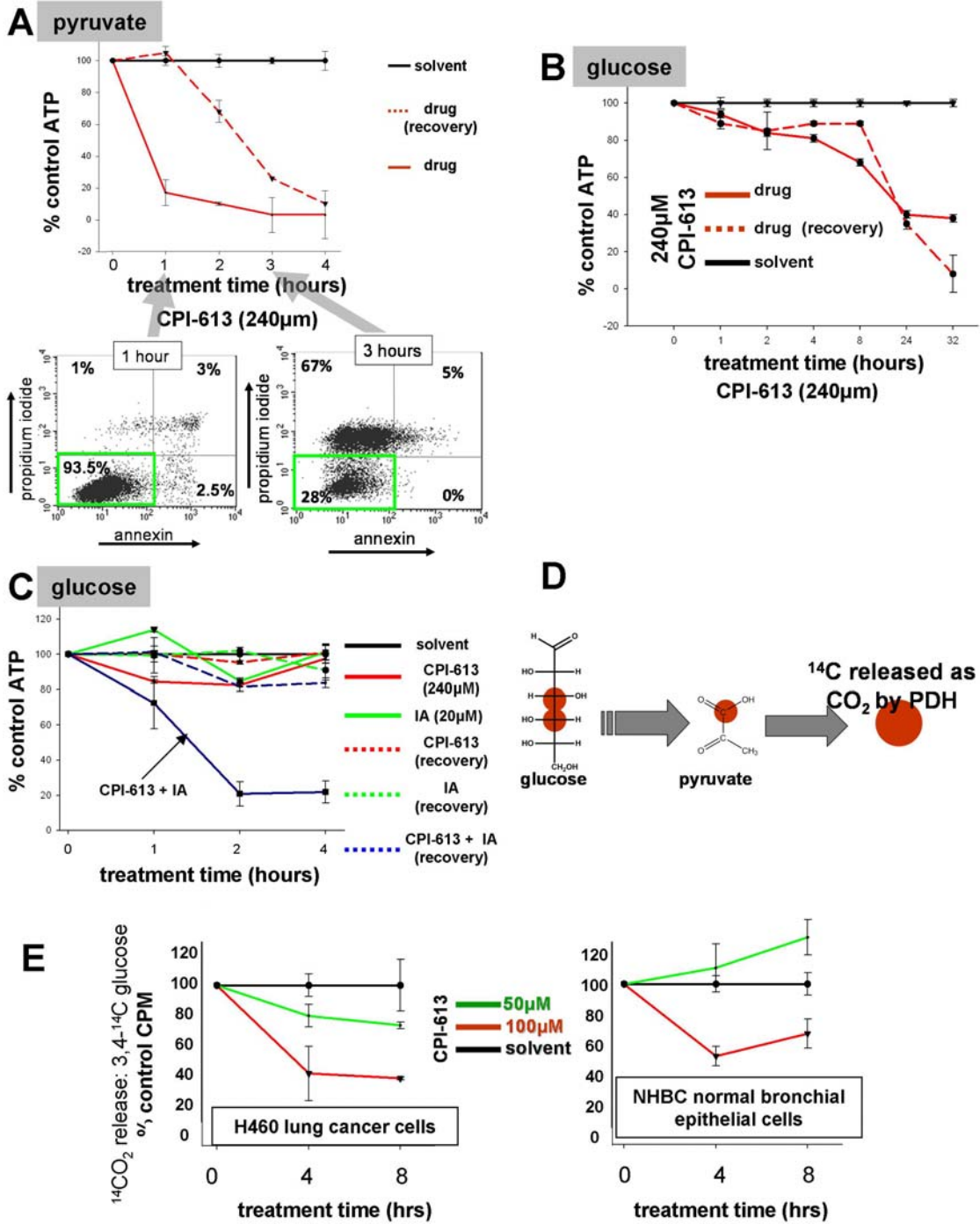


Figure 3

Figure 3: *CPI-613 disrupts H460 cancer cell mitochondrial metabolism including inhibition of PDH complex activity.* **a.** Shows reduction in ATP levels and commitment to death in H460 cancer cells induced by CPI-613 in pyruvate-glutamine medium. Solid lines are treatment for indicated times. Dashed lines are the same treatment times followed by three hours of recovery in drug-free medium. At bottom are the results of FACS analysis of propidium iodide uptake and annexin staining analysis of cell death (live cells in green-boxed quadrant). **b.** Shows induction of commitment to cell death as in panel a except in glucose-containing medium (RPMI). **c.** Shows iodoacetate (IA) sensitization to CPI-613 reduction in ATP levels in glucose medium assayed as in panel a. **d.** Diagrams radiolabeled glucose used in panel e. Red circles indicate ^{14}C label. Glucose C-3 and C-4 both become pyruvate C-1 through glycolysis. **e.** Shows oxidative release of ^{14}C as CO_2 from C-3,4 labeled glucose catalyzed by PDH in H460 lung cancer cells and NHBC normal bronchial epithelial cells. Both cells lines were cultured in the low serum medium recommended for NHBC cells, resulting in higher effective potency of CPI-613 (EC_{50} of ca. $50\mu\text{M}$, Figure 2a).

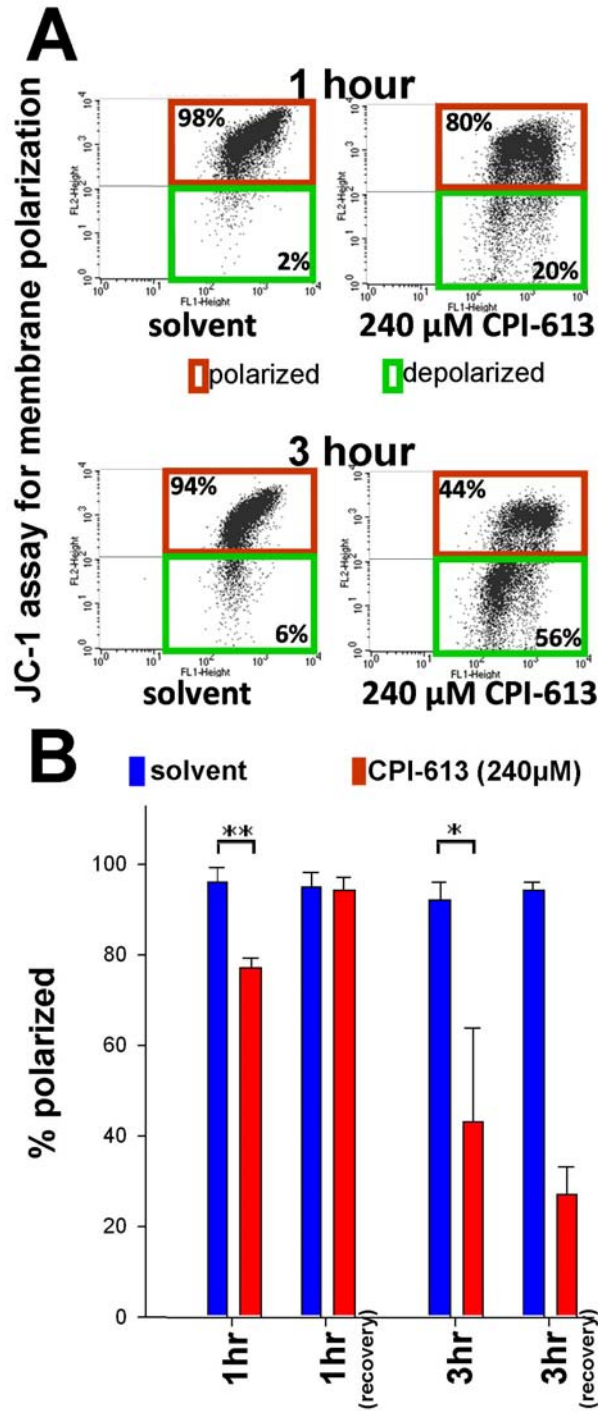


Figure 4

Figure 4: *CPI-613 treatment causes loss of mitochondrial membrane potential as assessed by JC-1 mitochondrial uptake.* **a.** Shows representative data points from FACS analysis of mitochondrial depolarization in H460 cell treated with CPI-613 for two different times in pyruvate-glutamine medium. **b.** Plots quantification of results of this assay. Note rapid and initially reversible loss of mitochondrial membrane potential. Recovery samples were incubated for three hours in drug-free medium after treatment, as in Figure 3a. Results are representative of at least three independent experiments. * $p < 0.04$; ** $p < 0.008$.

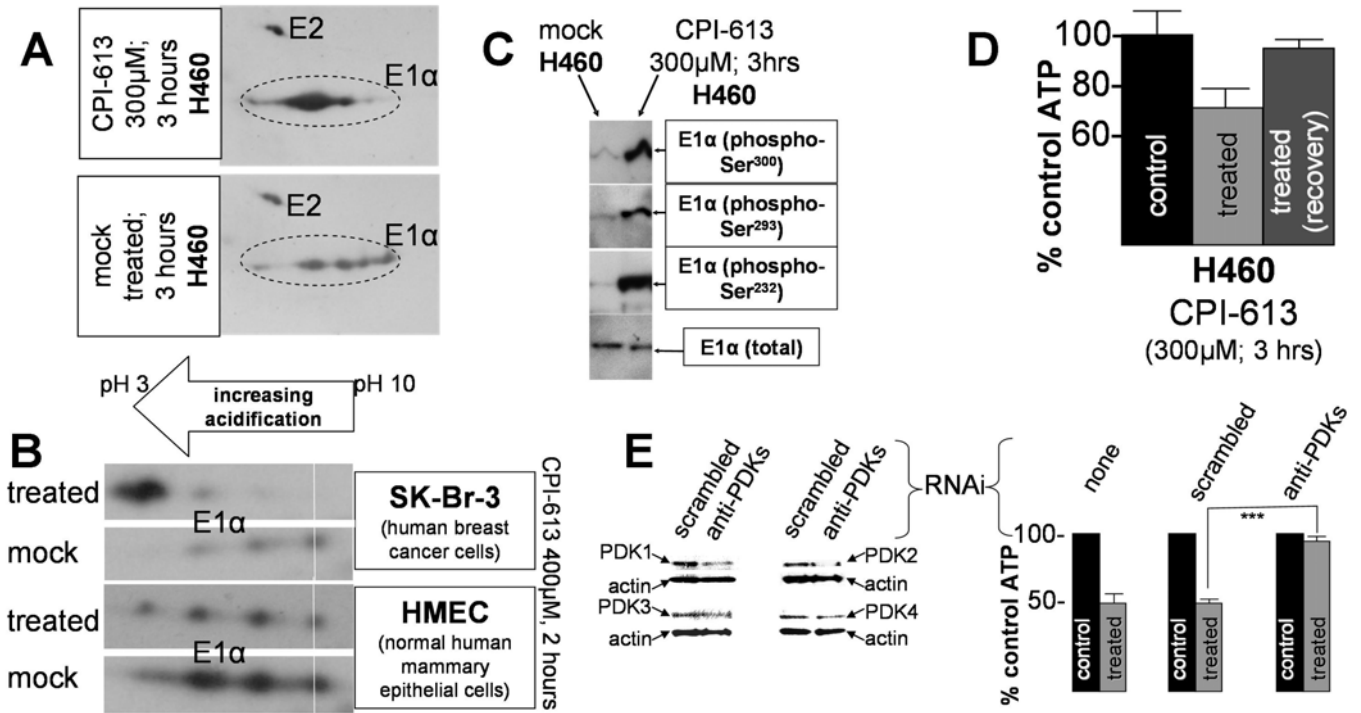


Figure 5

Figure 5: *CPI-613 induces extensive post-translational modification of PDH E1 and high PDK levels are essential to CPI-613 response.* **a.** Shows two dimensional Western analyses of extracts from H460 lung cancer cells treated with CPI-613 or mock-treated. **b.** Shows enlargements of the E1 α portions of paired two-dimensional blots of CPI-613-treated and mock-treated samples (human breast cancer, SK-Br-3, and normal human mammary epithelial cells, HMEC). Vertical white lines indicate the position of the non-phosphorylated, enzymatically active form of E1 α . **c.** Shows one-dimensional Western analysis of CPI-613 induction of three specific lipocate-sensitive PDK-dependent E1 α phosphorylation events (samples as in panel a). **d.** Shows ATP levels in H460 cells processed as for the Western samples in panels a and c. Levels were analyzed at treatment times indicated [treated] or after an additional three hours of recovery in drug-free medium [treated (recovery)]. **e.** Shows results of simultaneous RNAi knockdowns of all four PDKs in H460 cancer cells. At left is Western analysis of the normalized level of PDK protein reduction (PDK1=40% reduction; PDK2=85%; PDK3=55%; PDK4=75%). At right is the effect of these knockdowns on H460 cell death response to CPI-613 assayed after 17 hours of treatment with 200 μ M drug. Transfection with PDK RNAi's results in ca. 40% cell number reduction. The drug response is normalized to the mock drug treated control. *** indicates $p < 0.001$. All results are representative of at least three independent experiments.

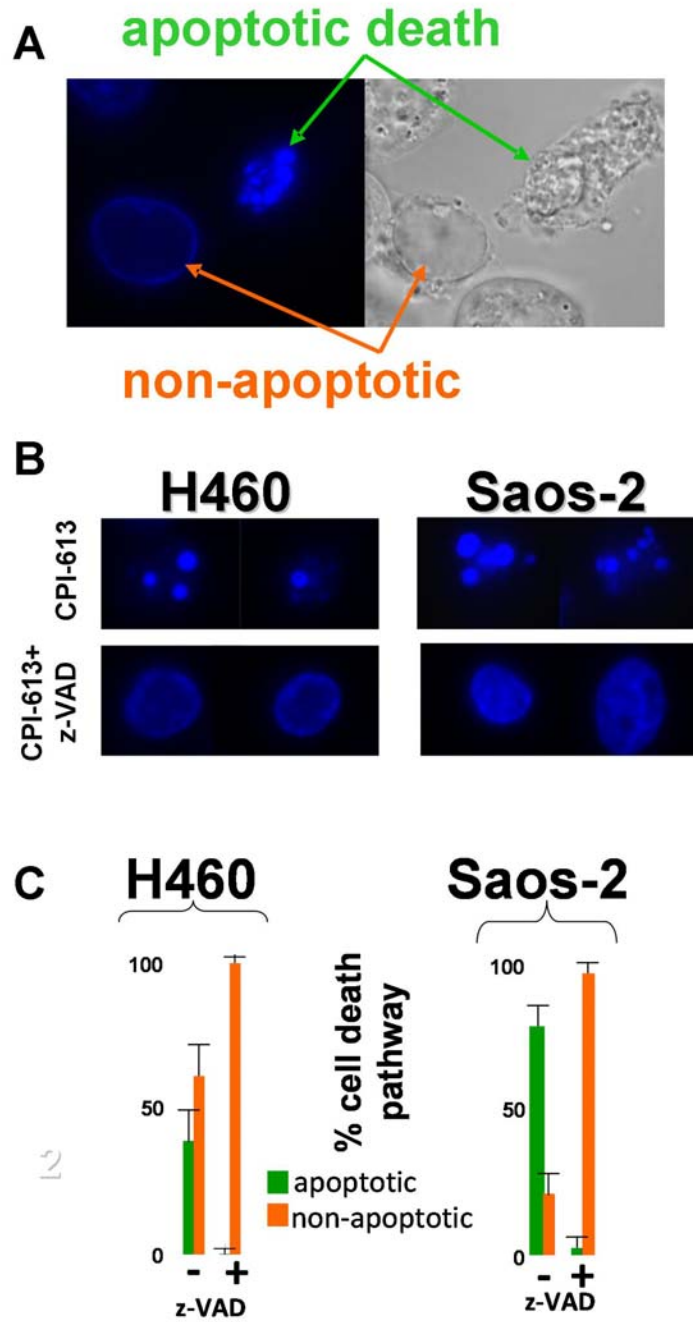


Figure 6

Figure 6: *CPI-613 induces both apoptotic and non-apoptotic cell death in H460 human lung cancer and Saos-2 human sarcoma cells.* **a.** Shows H460 cells treated with 240 μ M CPI-613 for 22 hours in glucose/RPMI. Two cells are in the late stages of cell death (arrows). One of the dying cells is undergoing apoptosis and the other non-apoptotic death. Also see cell death movies in Supplemental Material. **b.** Shows representative nuclei from fields of H460 or Saos-2 cells treated with 240 μ M CPI-613 for 24 hours in the presence or absence of the caspase/apoptosis inhibitor z-VAD-FMK. **c.** Shows results of quantification of apoptotic and non-apoptotic cell death induced by CPI-613 treatment of H460 and Saos-2 cells in the presence and absence of z-VAD-FMK as in panel b. Statistics in panel c reflect counts from three independent experiments aggregated as described in Supplemental Material.

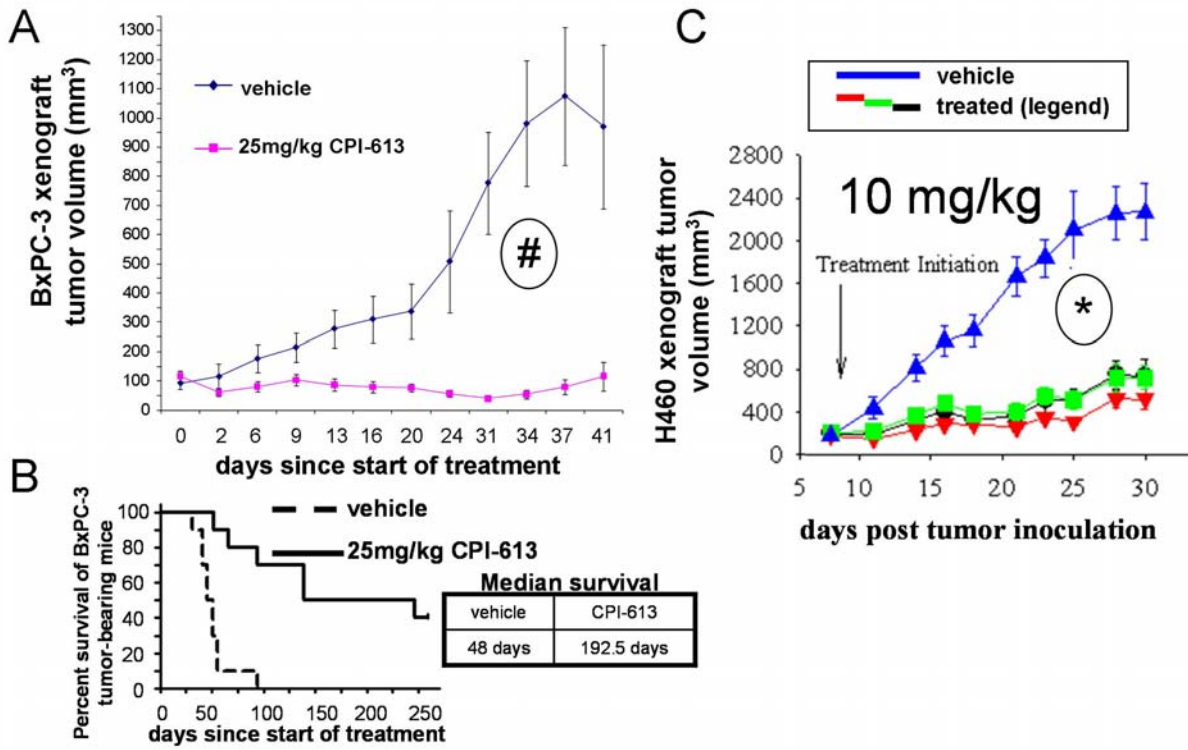


Figure 7

Figure 7: *CPI-613 is a potent inhibitor of human xenograft tumor growth.* **a.** Shows a human pancreatic (BxPC-3) xenograft carrying animal set injected once weekly with CPI-613 at 25mg/kg or with the vehicle control. After four treatments at seven day intervals, dosing was suspended and tumor residues were examined for regrowth for an additional 21 days. **b.** Shows long-term survival in BxPC-3 bearing animals treated as in panel a. Animals were euthanized as prescribed by IACUC regulations when tumor burden became large or when animals showed signs of poor health for other reasons. **c.** Shows H460 human lung tumor carrying animal sets injected with 10mg/kg CPI-613 once weekly (black circles), three times weekly (red triangles), or five times weekly (blue triangles for vehicle treatment and green squares for CPI-613 treatment). Statistics: # - p value for differences from the control at 37 days after initiation of treatment is ca. 0.00103. * - p values for differences from the control at 30 days after initiation of treatment are ca. 0.000204, 0.000053 and 0.000087 for 1X weekly, 3X weekly and 5X weekly dosing, respectively.